Supplementary Materials for

The strength of tumor reactivity is uncoupled from clonal expansion among TIL-derived TCRs

Shian Ouyang# [1], Zihan Zhao# [1, 2], Siyang Liu[2], Shichen Ma[1], Xiangyu Wu[2], Mingxin Fan[1], Ning Jiang[2], Rong Yang[2], Jie P. Li* [1]

1. State Key Laboratory of Coordination Chemistry, Chemistry and Biomedicine Innovation Center (ChemBIC), School of Chemistry, Nanjing University, Nanjing 210033, China;
2. Department of Urology, Affiliated Drum Tower Hospital, Medical School of Nanjing University, Nanjing 210008, China;

# These authors contributed equally.

* Corresponding author: jieli@nju.edu.cn

This supplementary materials file includes:

Supplementary Figures: S1 to S3

Other supplementary materials for this manuscript:

Table S1

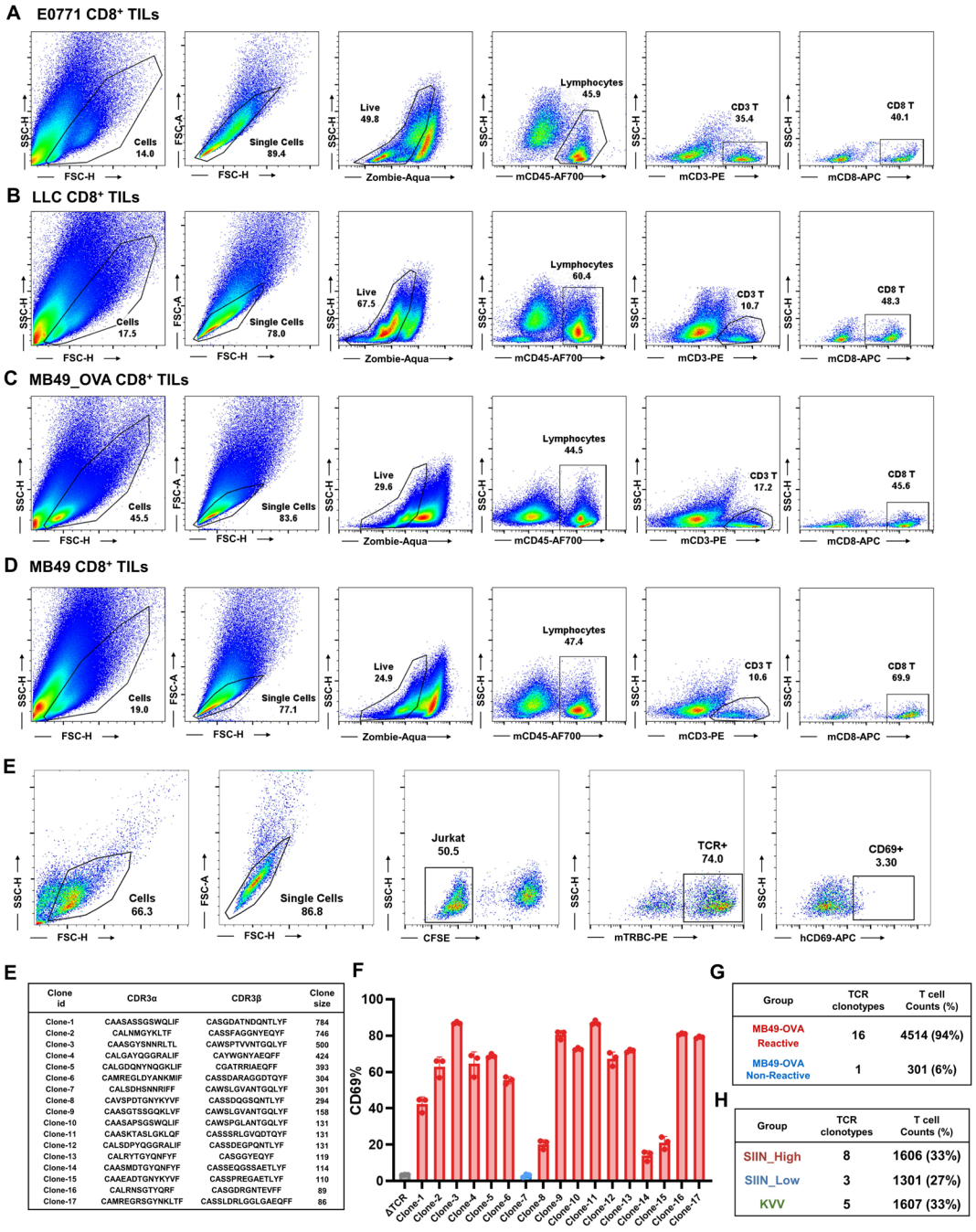

E

Clone id	CDR3α	CDR3β	Clone size
Clone-1	CAASASSGSWQLIF	CASGDATNDQNTLYF	784
Clone-2	CALNMGYKLTF	CASSFAGGNYEQYF	746
Clone-3	CAASGYSNNRLTL	CAWSPTVVNTGQLYF	500
Clone-4	CALGAYQGGRALIF	CAYWGNYAEQFF	424
Clone-5	CALGDQNYNQGKLIF	CGATRRIAEQFF	393
Clone-6	CAMREGLDYANKMIF	CASSDARAGGDTQYF	304
Clone-7	CALSDHSNNRIFF	CAWSLGVANTGQLYF	301
Clone-8	CAVSPDTGNYKYVF	CASSDQGSQNTLYF	294
Clone-9	CAASGTSSGQKLVF	CAWSLGVANTGQLYF	158
Clone-10	CAASAPSGSWQLIF	CAWSPGLANTGQLYF	131
Clone-11	CAASKTASLGKLQF	CASSSRLGVQDTQYF	131
Clone-12	CALSDPYQGGRALIF	CASSDEGPQNTLYF	131
Clone-13	CALRYTGYQNFYF	CASGGYEQYF	119
Clone-14	CAASMDTGYQNFYF	CASSEQGSSAETLYF	114
Clone-15	CAAEADTGNYKYVF	CASSPREGAETLYF	110
Clone-16	CALRNSGTYQRF	CASGDRGNTEVFF	89
Clone-17	CAMREGRSGYNKLTF	CASSLDRLGGLGAEQFF	86

F

G

Group	TCR clonotypes	T cell Counts (%)
MB49-OVA Reactive	16	4514 (94%)
MB49-OVA Non-Reactive	1	301 (6%)

H

Group	TCR clonotypes	T cell Counts (%)
SIIN_High	8	1606 (33%)
SIIN_Low	3	1301 (27%)
KVV	5	1607 (33%)

Figure S1. Flow-cytometric characterization of TILs and validation of the top expanded MB49-OVA clonotypes

(A–C) Representative flow cytometry gating strategy for isolating CD8⁺ TILs from E0771 (A), LLC (B), and MB49-OVA (C) tumors.

(D) Representative flow cytometry plots for the Jurkat–tumor co-culture assay used for functional validation. Tumor cells were pre-labeled with CFSE to distinguish them from Jurkat cells, after which TCR-positive Jurkat cells were gated and their activation status was assessed by CD69 induction.

(E) Table listing the top 17 expanded clonotypes recovered from MB49-OVA CD8⁺ TILs, including paired CDR3α/CDR3β sequences and clonotype sizes.

(F) Quantification of CD69 induction in Jurkat cells expressing each of the top 17 TCRs after co-culture with MB49-OVA tumor cells. ΔTCR Jurkat cells served as the negative control (gray).

Reactive and non-reactive clonotypes are shown in red and blue, respectively. Reactivity was defined as $CD69^+ \geq 10\%$. Data are shown as mean ± SEM from n = 3 independent co-culture experiments per group.

(G) Summary of validation outcomes among the 17 top expanded clonotypes, showing the numbers of reactive and non-reactive clonotypes and the corresponding T cell counts represented by these clonotypes in the scTCR-seq dataset.

(H) Summary of the validated reactive clonotypes grouped as SIIN_High, SIIN_Low, and KVV, including clonotype numbers and the corresponding T cell counts and fractions represented by each group in the scTCR-seq dataset.

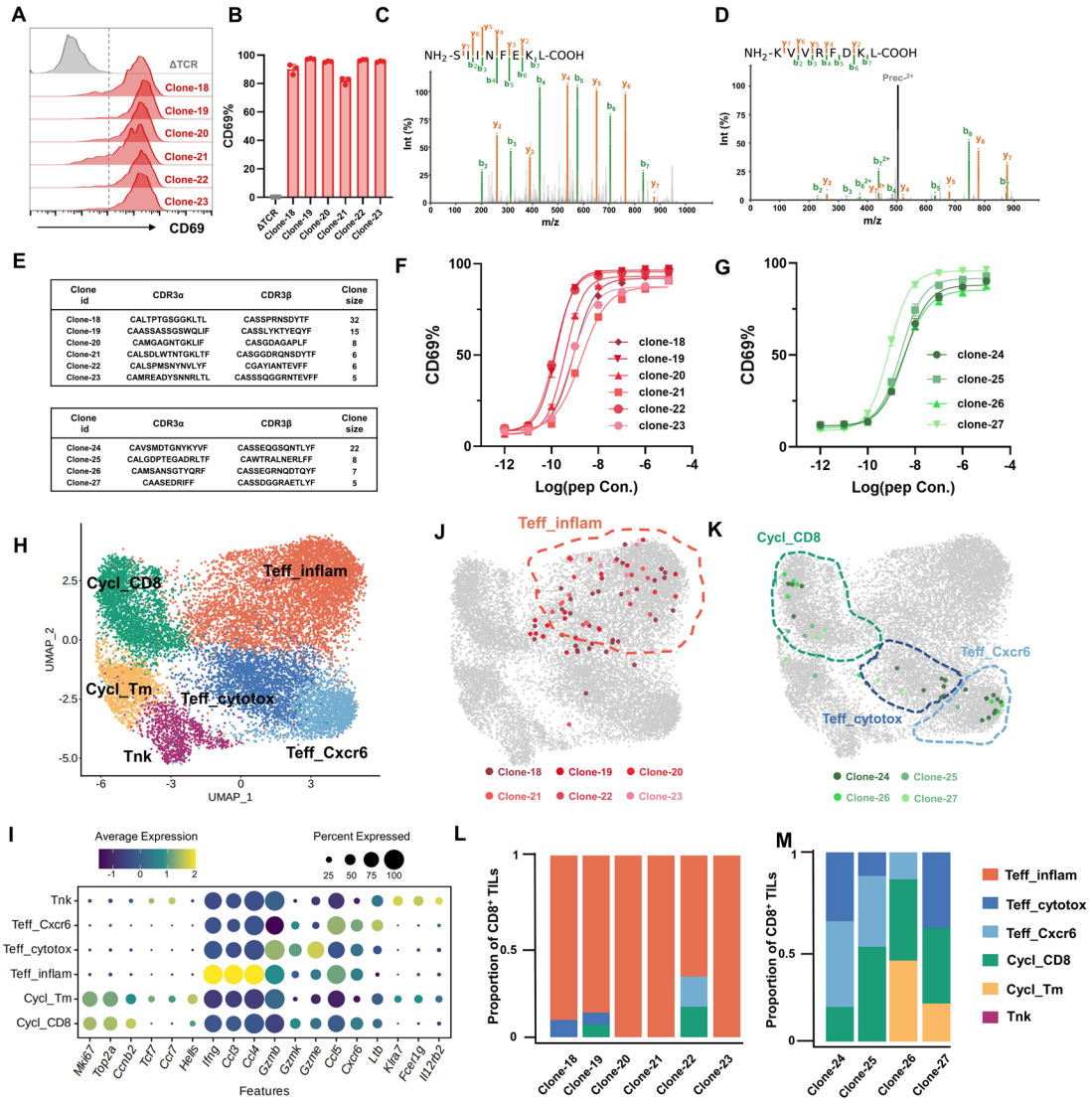

Figure S2. Characterization of low-frequency reactive TCRs in MB49-OVA CD8⁺ TILs

(A and B) Representative flow cytometry histograms (A) and quantification of CD69 induction (B) for low-frequency clonotypes identified from MB49-OVA CD8⁺ TILs after co-culture of TCR-transduced Jurkat cells with MB49-OVA tumor cells. Detailed clonotype information is provided in (E). Data are shown as mean ± SEM from n = 3 independent co-culture experiments per group.

(C and D) Representative MS/MS spectra supporting identification of SIINFEKL (C) and KVVRFDKL (D) from MB49-OVA immunopeptidomics.

(E) Table listing low-frequency reactive clonotypes assigned to the SIIN_High (Top) and KVV groups (Bottom), including paired CDR3α/CDR3β sequences and clonotype sizes.

(F and G) Peptide titration curves for TCR-transduced Jurkat cells co-cultured with H-2K^{b}-expressing MC38 cells at a 1:1 ratio for 18 h in the presence of serially diluted SIINFEKL or KVVRFDKL peptide (10^{-12} to 10^{-5} M). CD69 induction was quantified as CD69⁺ frequency. Data are shown as mean ± SEM from n = 3 independent peptide-stimulation experiments for each TCR.

(H) UMAP of MB49-OVA CD8⁺ TILs. Clusters are color-coded and labeled with inferred cell states. Teff_inflam was enriched for *Ccl3* and *Ccl4*, Teff_cytotox for cytotoxic genes including *Gzmb* and *Gzme*, Teff_Cxcr6 for *Cxcr6* and *Ccl5*, Cycl_CD8 for proliferation-associated genes including *Mki67* and *Top2a*, Cycl_Tm for cycling cells with partial stem-like features, including

Tcf7 and *Ccr7* expression and Tnk for high *Klra7* and *Fcer1g* expression. Marker expression is summarized in (I).

(I) Dot plot showing the expression of selected marker genes across the indicated transcriptional states in MB49-OVA $CD8^+$ TILs. Dot color indicates scaled average expression and dot size indicates the fraction of expressing cells.

(J and K) UMAP projections highlighting low-frequency reactive clonotypes assigned to the SIIN_High group (J) and KVV group (K). Colors denote individual clonotypes and other cells are shown in gray.

(L and M) Bar plots showing the transcriptional state composition of low-frequency reactive clonotypes in the SIIN_High group (L) and KVV group (M).

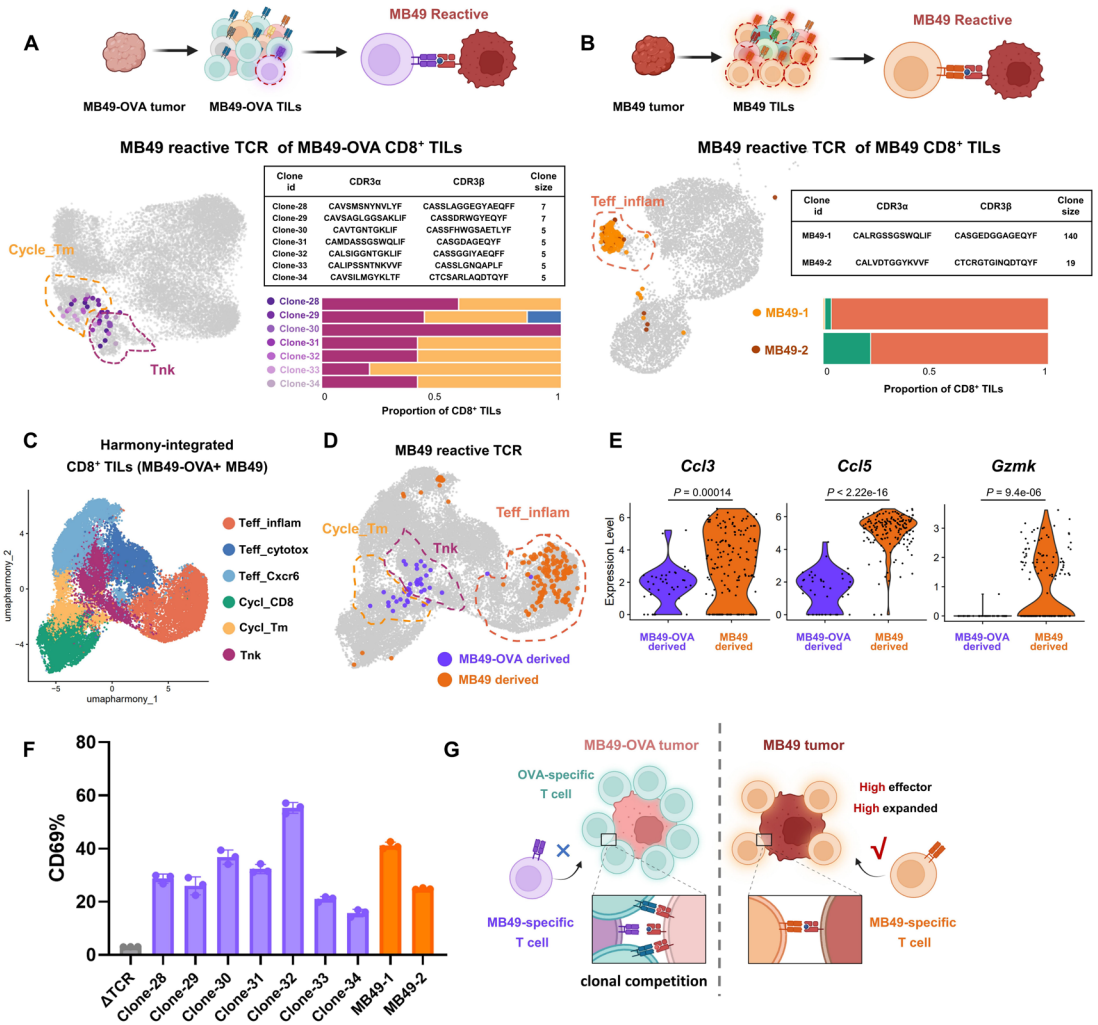

Figure S3. MB49-reactive clonotypes identified in MB49-OVA and parental MB49 CD8⁺ TILs

(A) UMAP of MB49-OVA CD8⁺ TILs scRNA-seq data with cells from MB49-reactive clonotypes highlighted (left). Colors denote distinct MB49-reactive clonotypes and other cells are shown in gray. The table (right, top) lists paired CDR3α/CDR3β sequences and clonotype sizes for MB49-reactive TCRs identified in MB49-OVA CD8 TILs. The stacked bar plot (right, bottom) shows the distribution of each MB49-reactive clonotype across transcriptional subsets.

(B) UMAP of parental MB49 CD8⁺ TILs scRNA-seq data with cells from MB49-reactive clonotypes highlighted (left). Colors denote distinct MB49-reactive clonotypes and other cells are shown in gray. The table (right, top) lists paired CDR3α/CDR3β sequences and clonotype sizes for MB49-reactive TCRs identified in MB49 CD8⁺ TILs. The stacked bar plot (right, bottom) shows the distribution of each MB49-reactive clonotype across transcriptional subsets.

(C) Harmony-integrated embedding of MB49-OVA and MB49 CD8⁺ TIL scRNA-seq datasets.

(D) MB49-reactive clonotypes mapped onto the Harmony-integrated embedding, with MB49-OVA-derived MB49-reactive cells in purple and MB49-derived MB49-reactive cells in orange.

(E) Violin plots comparing expression of selected transcripts between MB49-OVA-derived and MB49-derived MB49-reactive cells, including *Ccl3*, *Ccl5*, and *Gzmk*. Each point represents one clonotype-matched CD8⁺ TIL. *P* values were calculated by two-sided Wilcoxon rank-sum tests and are shown in the plots.

(F) Quantification of CD69 induction in Jurkat cells expressing individual MB49-reactive TCRs after co-culture with MB49 tumor cells. ΔTCR Jurkat cells served as the negative control and are shown in gray. TCRs isolated from MB49-OVA and parental MB49 tumors are shown in purple and orange, respectively. Data are shown as mean ± SEM from n = 3 independent co-culture experiments per group.
(G) Working model illustrating that immunodominant OVA-specific responses in MB49-OVA can limit signal-1 access for MB49-specific T cells via clonal competition (left), whereas in parental MB49 tumors the absence of OVA-specific competition permits stronger signal 1, higher expansion, and more effector-like programs (right).
Parts A, B and G were created using BioRender.